

# EXTRACTION OF TRAFFIC ISLANDS VIA ACTIVE CONTOURS WITHOUT EDGES

M. Ravanbakhsh, C.S. Fraser, M. Awrangjeb

Cooperative Research Center for Spatial Information, Department of Geomatics  
University of Melbourne VIC 3010, Australia  
[m.ravanbakhsh, c.fraser, mawr]@unimelb.edu.au

Commission III - WG III/4

**KEY WORDS:** Feature extraction, road junction, traffic island, active contour, high resolution, aerial image

## ABSTRACT:

Within topographic databases, traffic islands constitute important features of mapped road networks. However, they are generally not explicitly modelled in most approaches to road extraction from aerial imagery. Traffic islands can be considered as elements of road junctions and in this paper an active contour-based approach for their automatic extraction is proposed. The road junction outline and vector data is first provided so attention can be focussed on specific locations. Constraints are then introduced to distinguish traffic islands from other features such as cars. Following a review of the active contour model adopted, and a description of the traffic island extraction approach, an account is given of experimental testing of the developed method. The testing utilised aerial images of 0.1 m ground resolution, over both suburban and rural areas. Experimental results are presented and prospects for the new approach are discussed.

## 1. INTRODUCTION

One of the trends accompanying the increased adoption of digital aerial cameras has been acquisition of imagery at increasingly higher spatial resolutions. This is affording more detailed extraction of topographic objects from imagery. Among man-made objects, road networks are of special importance as they are used in such a wide variety of applications. Road junctions are important components of a road network. However, they are typically not explicitly modelled in existing road extraction approaches. Within road network extraction systems, road junctions have mainly been modelled as point objects where three or more road segments meet (Gerke, 2006; Zhang, 2003; Barsi et al., 2002; Wiedemann, 2002 and Hinz, 1999). Junctions have also been treated as planar objects (Gautama et al., 2004; Mayer et al., 1998 and Heipke et al., 1995). Of the approaches referenced, none attempt to model small traffic islands, which are often present in the central area of junctions. Thus, the degree of detail demanded at larger mapping scales is not reflected in the final vector data, as exemplified in Fig. 1.

Ravanbakhsh et al. (2008; 2009) previously presented a detailed junction model and an approach for the automatic extraction of both traffic islands in complex, multi-island junctions and central islands in roundabouts. For roundabouts, a hybrid level-sets evolution strategy was used to extract the central islands. In this strategy, which requires a high number of iterations, the initial curves located inside and outside the central island evolve towards the boundaries of the central island. For complex junctions, where small islands exist, the image is segmented based on a clustering technique under the assumption that the image contains two classes of objects, namely the road and the island surface. Level sets are then initialized and they evolve to detect the island boundaries. The intermediate results obtained are subject to geometric and topological constraints in order to remove non-island features. Level sets cannot detect smooth boundaries, which frequently occur in traffic islands, as they are smoothed before level set

evolution. Furthermore, this approach is largely dependent on the segmentation so that islands classified as road surface in the segmentation cannot be recovered.

In this paper, traffic islands are modelled as necessary components of road junctions and an active contour-based approach for their automatic extraction is proposed. The outline of the road junction, as well as vector data, are used as input to allow attention to be focussed upon a specific, limited area. Furthermore, selected geometrical and topological constraints are defined to distinguish islands from other features.



Figure 1. Road vector data overlaid on a high-resolution aerial image.

## 2. ACTIVE CONTOUR MODEL

Unlike simple road junctions, complex junctions can contain several traffic islands located in their central area. The number and size of islands varies depending upon the number of crossing roads and the junction's functionality. Whereas in complex junctions islands are often of small size, roundabouts as a subclass of complex junctions, contain a large central island. Traffic islands are of diverse geometrical shape, and they can be partially occluded in aerial images by shadows from traffic lights, signage and vehicles. These properties imply that the extraction of islands is a challenging problem in aerial image analysis.

Furthermore, the number of islands in a junction may be unknown. Therefore, it is crucial to be able to handle a change of topology of the curve that is to delineate islands. Level sets can provide a solution to this problem of a required change in

topology. However, level sets based on the edge gradient function are unable to capture the smooth boundaries that frequently characterize island borders. In previous work (Ravanbakhsh et al., 2008; 2009), two different level set initialization strategies were proposed for small and central islands. In the approach proposed here, however, an active contour model that is both independent of edge gradients and flexible in initialization is used in an effort to overcome limitations found with the previous strategy. The active contour model adopted is based on techniques of curve evolution and level sets.

Let  $u_0$  be a given image and  $C$  the evolving curve, with  $c_1$  and  $c_2$  denoting two constants representing the averages of  $u_0$  inside and outside the curve  $C$ . This model covers the minimization of an energy based segmentation. Assume that the image  $u_0$  is formed by two regions of approximately piecewise-constant intensities with distinct values of  $u_0^i$  and  $u_0^o$ , and that the object to be detected is represented by the region with value  $u_0^i$  and boundary  $C$ . Then,  $u_0 \approx u_0^i$  inside the object (inside  $C$ ) and  $u_0 \approx u_0^o$  outside the object (outside  $C$ ). By minimizing the following energy equation, the boundary of the object of interest  $C$  is obtained (Chan and Vese, 2001):

$$F_1(C) + F_2(C) = \int_{\text{inside}(C)} |u_0 - c_1|^2 dx dy + \int_{\text{outside}(C)} |u_0 - c_2|^2 dx dy \quad (1)$$

Eq. (1) is regularized by adding two terms for the length of  $C$  and the area inside  $C$ :

$$F(C, c_1, c_2) = \mu \cdot \text{length}(C) + \nu \cdot \text{area}(\text{inside } C) + \lambda_1 \int_{\text{inside}(C)} |u_0 - c_1|^2 dx dy + \lambda_2 \int_{\text{outside}(C)} |u_0 - c_2|^2 dx dy \quad (2)$$

where  $\mu > 0$ ,  $\nu \geq 0$ ,  $\lambda_1, \lambda_2 > 0$  are fixed parameters. Eq. (2) can be formulated and solved in a level-sets framework in order to handle automatic changes of topology so that unknown numbers of objects can be detected simultaneously. The core idea of level sets is to implicitly represent a curve  $C$  as the zero level curve of a function  $\phi$  of higher dimension. Under the assumption that  $C$  represents the boundary between two regions, one region inside the curve and another outside the curve,  $\phi$  is defined as the signed distance  $\pm d(x)$  to the curve, negative outside and positive inside (see Ravanbakhsh et al., 2008 for a description of level sets). To transform Eq. (2) into level sets,  $C$  is replaced by  $\phi$ , leading to the new energy function

$$F(\phi, c_1, c_2) = \mu \cdot \text{length}\{\phi=0\} + \nu \cdot \text{area}\{\phi \geq 0\} + \lambda_1 \int_{\phi \geq 0} |u_0 - c_1|^2 dx dy + \lambda_2 \int_{\phi < 0} |u_0 - c_2|^2 dx dy \quad (3)$$

The length term obtained by taking the surface integral (line in  $\mathbb{R}^2$ ) over the curve  $C$  in a specified computational domain  $\Omega \subset \mathbb{R}^2$  is given by

$$\text{length}\{\phi=0\} = \int_{\Omega} |\nabla H(\phi)| dx dy = \int_{\Omega} \delta(\phi) |\nabla \phi| dx dy \quad (4)$$

where  $H$  denotes the Heaviside function

$$H(\phi) = \begin{cases} 0 & \text{if } \phi < 0 \\ 1 & \text{if } \phi \geq 0 \end{cases} \quad (5)$$

and  $\delta$  denotes the univariate Dirac delta function

$$\delta(\phi) = \begin{cases} \infty & \text{if } \phi = 0 \\ 0 & \text{if } \phi \neq 0 \end{cases} \quad (6)$$

The area term is obtained by computing the volume integral

(area in  $\mathbb{R}^2$ ) of the interior region (Osher & Fedkiw, 2002)

$$\text{area}\{\phi \geq 0\} = \int_{\Omega} H(\phi) dx dy \quad (7)$$

The last two energy terms in Eq. (3) are rewritten as

$$\lambda_1 \int_{\phi \geq 0} |u_0 - c_1|^2 dx dy = \int_{\Omega} |u_0 - c_1|^2 H(\phi) dx dy \quad (8)$$

$$\lambda_2 \int_{\phi < 0} |u_0 - c_2|^2 dx dy = \int_{\Omega} |u_0 - c_2|^2 H(-\phi) dx dy \quad (9)$$

Then, the energy  $F(\phi, c_1, c_2)$  in Eq. 3 can also be rewritten:

$$F(\phi, c_1, c_2) = \mu \int_{\Omega} |\nabla H(\phi)| dx dy + \nu \int_{\Omega} H(\phi) dx dy + \int_{\Omega} |u_0 - c_1|^2 H(\phi) dx dy + \int_{\Omega} |u_0 - c_2|^2 H(-\phi) dx dy \quad (10)$$

With  $\phi$  fixed and a minimization of the energy  $F(C, c_1, c_2)$  with respect to the constants  $c_1$  and  $c_2$ , expressions for constants  $c_1$  and  $c_2$  follow as

$$\begin{cases} c_1(\phi) = \frac{\int_{\Omega} u_0 H(\phi) dx dy}{\int_{\Omega} H(\phi(x, y)) dx dy} \\ c_2(\phi) = \frac{\int_{\Omega} u_0 H(-\phi) dx dy}{\int_{\Omega} H(-\phi(x, y)) dx dy} \end{cases} \quad (11)$$

Eq. 10 is solved using a calculus of variation approach (Courant & Hilbert, 1953). The Gateaux derivative (first variation) of the functional  $F$  in Eq. 9 can be written as

$$\frac{\partial \phi}{\partial t} = -\delta(\phi) \left[ \mu \operatorname{div} \left( \frac{\nabla \phi}{|\nabla \phi|} \right) - \nu - \lambda_1 (u_0 - c_1)^2 + \lambda_2 (u_0 - c_2)^2 \right] \quad (12)$$

The function  $\phi$  that minimizes this functional satisfies the Euler-Lagrange equation  $\partial F / \partial \phi = 0$ . The steepest descent process for minimization of the functional  $F$  is the following gradient flow (Chan and Vese, 2001):

$$\frac{\partial \phi}{\partial t} = \delta(\phi) \left[ \mu \operatorname{div} \left( \frac{\nabla \phi}{|\nabla \phi|} \right) - \nu - \lambda_1 (u_0 - c_1)^2 + \lambda_2 (u_0 - c_2)^2 \right] \quad (13)$$

This gradient flow is the evolution equation of the active contour used in the proposed extraction approach. In all experiments, control parameters are set as  $\nu = 0.5$ ,  $\mu = 0.4$  and  $\lambda_1 = \lambda_2 = 1$ . Use of a larger time step can speed up the evolution, but may cause error in the boundary location if the chosen time step is too large. In this paper  $\partial t = 0.5$  has been used.

### 3. EXTRACTION APPROACH

In the present development, use is made of junction outlines obtained using an automatic approach for road junction extraction (Ravanbakhsh et al., 2008). This component, along with vector data and the aerial imagery, is regarded as input. The proposed strategy for each island then comprises three steps, as indicated in Fig. 2. First, the island area is clipped from the image and pre-processed. Second, the island boundary is detected and, finally, detected non-island features are eliminated and the selected boundary curves are post-processed to yield the extracted island.

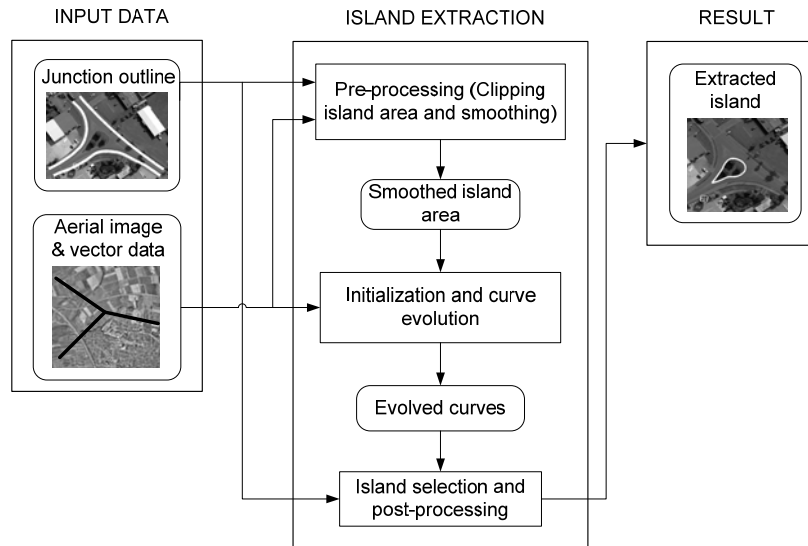


Figure 2. Workflow for traffic island extraction.

### 3.1 Pre-processing

In an initial step, the junction outline where islands are located is clipped from the image. The search space for islands is further restricted to an area around the estimated junction centre point with the size of  $80 \times 80 \text{ m}^2$  ( $800 \times 800$  pixels) (Fig. 3a). This is called the island area. Before the evolution begins, the island area is pre-processed to remove fine-detail disturbing features. First, a morphological opening operator with a circular structure element of size 7 pixels is applied in order to remove distortions such as road markings. This is followed by application of a closing operator with the same structure element to eliminate small shadows. Finally, a Gaussian smoothing operator with a sigma value of 10 is applied (Fig. 3b).

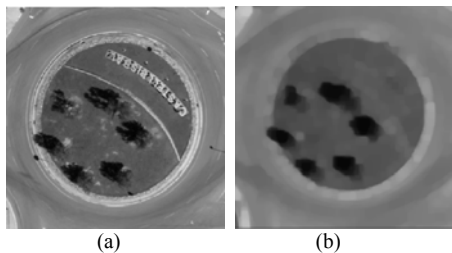


Figure 3. (a) Island area is clipped using vector data, and (b) pre-processing result is shown after morphology opening and closing operators are applied.

### 3.2 Initialization and curve evolution

To begin the curve evolution, the initial level set function needs to be constructed. This commences with a square-shaped contour so that areas enclosed by the contour are assigned a positive constant value, while areas outside the contour are assigned a negative value of the same magnitude, namely 1.2 (Fig. 4a, e). Initialization in this active contour model is quite flexible as the quadrilateral curve can be situated anywhere within the island area. Shown in Fig.4 are two cases where initial curves are located inside (Fig. 4b) and outside (Fig. 4f) the central island. In both cases, final curves have converged precisely to the object boundary. The initial level set function will evolve according to the evolution equation, Eq. 13, with its zero level curve converging to the exact boundary of the island.

The curve evolution is terminated when the overall change in the evolving curve positions per iteration is less than 1 pixel.

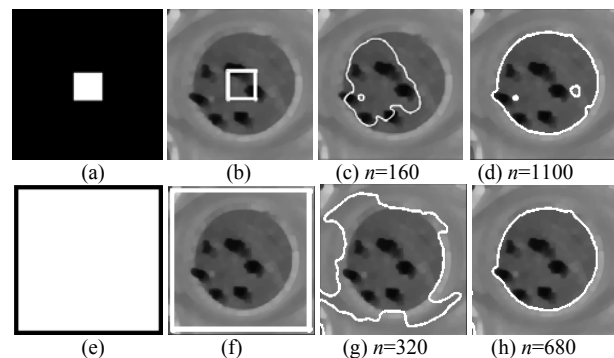


Figure 4. Initialization and curve evolution, with  $n$  denoting the number of iterations: (a) initial level set function; (b) initial curve situated inside the island; (c) intermediate result of curve evolution; (d) evolved curve; (e) initial level set function; (f) initial curve located outside the island; (g) intermediate result; (h) evolved curve.

One of the main advantages of the active contour employed is that it can detect objects with smooth boundaries since it is independent of edge gradients. This property can be observed in Fig. 5 where the island comprises a smooth boundary, yet this boundary can still be detected and accurately delineated.

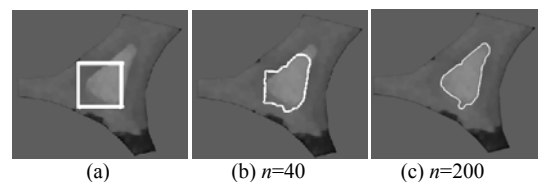


Figure 5. Curve evolution result for weak boundaries: (a) initialization; (b) evolving curve; (c) final curve.

### 3.3 Island selection and post-processing

The result of the evolution is a set of curves converged to existing features inside the junction. In order to remove the non-island curves, geometric and topological constraints are introduced based on the properties of islands, because, in addition to the islands, some undesirable features such as

vehicles might be extracted as candidate islands. Small closed areas such as cars are easily removed as their areas are below a certain threshold (Fig. 6-b).

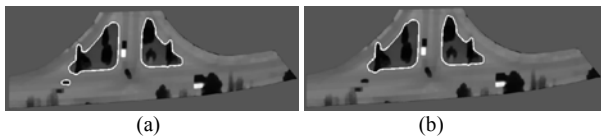


Figure 6. (a) Evolved curves; (b) Detected vehicle is removed.

Since island candidates must be located within the junction outline, those curves that lie on the junction outline are removed. Since islands possess boundaries with a small curvature variation, so the contours with high curvature variations, i.e. their mean curvature is greater than a certain threshold, are eliminated. A further constraint is applied only on central islands as they are the largest areas detected within the computation domain. As a result, their selection is rather straightforward. Selected curves for small traffic islands are smoother. For central islands in roundabouts, a best-fit ellipse is computed via least-squares (Fig. 7).

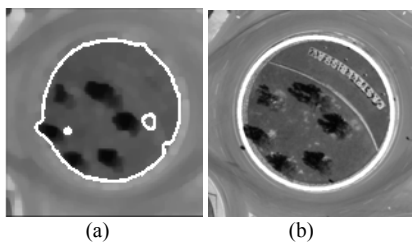


Figure 7. (a) Curve evolution result; (b) Result after selection and ellipse fitting.

#### 4. EXPERIMENTAL EVALUATION

The proposed approach was tested on a set of complex road junction samples and roundabouts, the aerial imagery having a ground sample distance of 0.1m. Results, as shown in Fig. 8, are presented here to highlight the potential of the new approach. As can be seen in the figure, different shapes and sizes of traffic islands can be recovered. However, one small island in Fig.8b (in the bottom centre) could not be extracted because its width was below a given threshold. Moreover, the geometry of other extracted small islands has not been captured precisely. The reason for this shortcoming is that the morphological operators cause the size of the island to decrease. As a result, the narrow parts of the islands are almost washed out. In Fig. 8e, two islands have been separately and correctly detected, whereas in the similar example of Fig. 8f, the two islands are merged due to the shadow cast between them.

In order to evaluate the performance of the approach, automatically extracted islands were compared to a reference data set of manually digitized islands which comprised 23 road junctions with 34 traffic islands. The comparison was carried out by matching the extracted islands to the reference data using the so-called “buffer method” (Heipke et al., 1998). The buffer width can be defined according to the required extraction accuracy for a specific application. It was decided to set a value of 0.5m (5 pixels) in order to evaluate the method for applications that require a high accuracy, such as car navigation. An extracted island was assumed to be correct if the maximum distance between the extracted island border and its corresponding reference border did not exceed the buffer width. Furthermore, a reference island border was assumed to be

matched if its maximum deviation from the extracted border was within the buffer width. Based on these assumptions, the following quality measures were adopted:

- **Completeness:** the ratio of the number of matched reference islands to the number of extracted islands.
- **Correctness:** the ratio of the number of correctly extracted islands to the number of extracted islands.
- **Geometrical accuracy:** the average distance between the correctly extracted island and the corresponding reference island, expressed as Root Mean Square (RMS) value.

Table 1 shows the evaluation result for the assigned buffer width of 5 pixels.

Number of islands	Completeness	Correctness	Geometrical accuracy
34	67 %	73 %	0.29m (3 pls)

Table 1. Evaluation results

While the results are encouraging, since most of islands have been extracted correctly, they illustrate that there are still some problems that the proposed approach cannot accommodate at this stage. These arise mainly in areas where a large number of vehicles and/or shadows exist. Tree shadows on the island border can cause the curve to lie somewhat outside the object boundaries, in which case the shadows are detected as a part of the island (Fig. 9c). Therefore, the result is incorrect. Similar situations can be seen in further samples where shadows affect the final result, as in Fig. 8f, and consequently the degree of correctness is degraded. A further problem area is poor contrast between the island surface and the surrounding asphalt area, in which case the island becomes radiometrically indistinct after pre-processing and so cannot be extracted, as illustrated in Fig. 9b. Pre-processing is as an essential step to remove small disturbing features. Nevertheless, in this step, islands with smaller sizes are washed out so they cannot be detected in later steps. This is the main reason why the Completeness measure is low for the test imagery.

The exploited active contour model is more effective in cases where two classes of objects with distinct radiometric properties exist. This assumption is equivalent to expecting that there are not too many disturbances such as cars or shadows in the junction, a requirement that is generally not fulfilled. Pre-processing can reduce the effect of disturbances to some extent, but it is not useful when road and island surfaces appear in the image with varying radiometric properties, as in Figs. 9d and 9e. The proposed approach has proven to be deficient in such situations.

#### 5. CONCLUDING REMARKS

A new approach for the automatic extraction from aerial imagery of traffic islands located within the central area of road junctions has been developed. The approach is based on an active contour model which is flexible in initialization and can detect islands with weak boundaries. The use of geometrical and topological constraints has proven to be useful in distinguishing traffic islands from other object features such as cars. Experimental application of the proposed approach has identified both its potential and some shortcomings, and further investigation into the integration of island shape information, and assignment of the internal energy of the active contour in order to overcome shadowing are desirable. Furthermore, use of colour information in a multi-phase active contour has the potential to overcome the problem of there being more than two

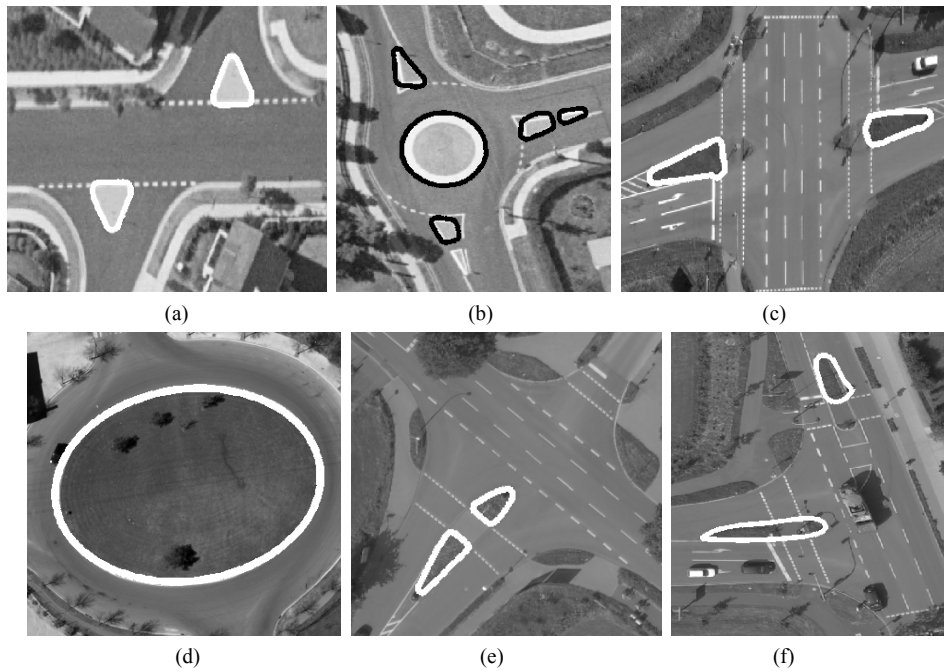


Figure 8. Sample traffic island extraction results.

classes of objects in the road junction. The initial detection of several classes of objects can also add to the complexity of the problem in the island selection step. In this case, further constraints need to be defined to distinguish between classes of objects. Or, as an alternative, other data sources such as precise height data could potentially be employed.

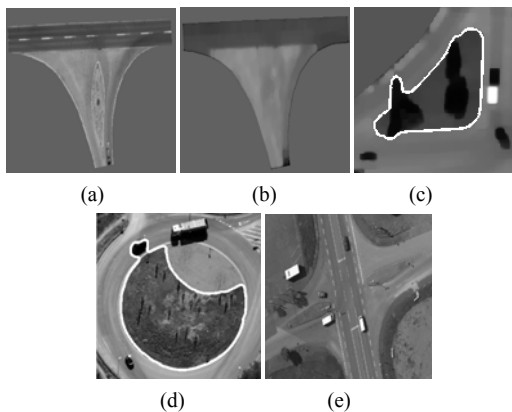


Figure 9. Failed and imprecise island extraction due to poor contrast (a, b), shadows (c) and heterogeneous road surface and islands (d, e).

## REFERENCES

Barsi, A., Heipke, C., Willrich, F., 2002. Junction Extraction by Artificial Neural Network System – JEANS. *International Archives of Photogrammetry and Remote Sensing* 34(B3), pp. 18-21.

Chan, T. F. and Vese, L. A., 2001. Active contours without edges. *IEEE Trans. on Image Processing* 10(2), pp. 266-277.

Courant, R., Hilbert, D., 1953. *Methods of Mathematical Physics*. Wiley-Interscience, New York.

Gautama, S., Goeman, W., D'Haeyer, J., 2004. Robust detection of road junctions in VHR images using an improved ridge detector. *International Archives of Photogrammetry and Remote Sensing* 35(B3), pp. 815-819.

Gerke, M., 2006. Automatic Quality Assessment of Road Databases Using Remotely Sensed Imagery. *Wissenschaftliche Arbeiten der Fachrichtung Geodäsie und Geoinformatik der Universität Hannover*, No. 261.

Heipke C., Mayer H., Wiedemann C., Jamet O., 1998. External evaluation of automatically extracted road axes, *Photogrammetrie Fernerkundung Geoinformation* 2, pp. 81-94.

Heipke, C., Steger, C., Multhammer, R., 1995. A hierarchical approach to automatic road extraction from aerial imagery. *McKeown D.M., Dowman I., (Eds.), Integrating Photogrammetric Techniques with Scene Analysis and Machine Vision II, SPIE Proceedings* 2486, pp. 222-231.

Hinz, S., Baumgartner, A., Steger, C., Mayer, H., Eckstein, W., Ebner, H., Radig, B., 1999. Road extraction in rural and urban areas. *Semantic Modeling for the Acquisition of Topographic Information from Images and Maps (SM-ATI'99)*, Munich, pp. 7-27.

Mayer, H., Laptev, I., Baumgartner, A., 1998. Multi-Scale and Snakes for Automatic Road Extraction. *Proceedings of Fifth European Conference on Computer Vision, Freiburg, Germany, Vol. 1406 of Springer Verlag Lecture Notes in Computer Science*, pp.720-733.

Osher, S., Fedkiw, R., 2002. *Level Set Methods and Dynamic Implicit Surfaces*. Springer-Verlag, New York.

Ravanbakhsh, M., Fraser, C.S., 2009. Road Roundabout Extraction from very high Resolution Aerial Imagery. *International Archives of Photogrammetry and Remote Sensing* 38(3/W4), pp. 19-26.

Ravanbakhsh, M., Heipke, C., Pakzad, K., 2008. Road junction extraction from high resolution aerial imagery. *The Photogrammetric Record* 23(124), pp. 405-423.

Ravanbakhsh, M., Heipke, C., Pakzad, K., 2008. Extraction of Traffic Islands from Aerial Images. *Photogrammetrie Fernerkundung Geoinformation* 5, pp. 375-384.

Wiedemann C., 2002. Improvement of Road Crossing Extraction and External Evaluation of the Extraction Results. *International Archives of Photogrammetry and Remote Sensing* 34(B3), pp. 297-300.

Zhang, C., 2003. Updating of Cartographic Road Databases by Images Analysis. Ph.D. thesis, Institute of Geodesy and Photogrammetry, ETH Zurich, Switzerland, IGP Mitteilungen No. 79.